A detailed analysis of the results indicates that for the compound nuclei formed in the Ra^{226} and lighter element reactions this average breaking distance is independent of the fragment mass ratio for a given mode. However, for the heavier compound nuclei, Pu^{231} and Pu^{237}, these measurements indicate that the average breaking distance for asymmetric mode fission increases slightly with increasing mass ratio. The magnitude of this variation with mass ratio is less than is obtained from measurements[8–10] of the total kinetic energy releases for thermal neutron-induced fission reactions. These differences indicate that the dependence of the average breaking distance on the fragment mass ratio is probably a function of both the mass or Z^2/A and the excitation energy of the compound nucleus.

However, the results indicate that at least for asymmetric mode fission the average breaking distance is only very slightly dependent on the excitation energy of the compound nucleus. For the symmetric mode the average breaking distances are found to be approximately independent of the excitation energy at moderate excitations but may be somewhat different for the lower excitation energy thermal neutron-induced fission.

For both modes the average breaking distance is found to increase as the mass of the compound nucleus increases.

ACKNOWLEDGMENTS

We gratefully acknowledge many helpful discussions with R. B. Leachman and J. J. Griffin on the interpretation of these results. Many helpful suggestions were also made by S. L. Whetstone, Jr., J. Terrell, J. H. Manley, and I. Halpern. We would like to thank J. C. D. Milton for performing calculations on the fission energetics for our reactions and S. L. Whetstone, Jr., for the use of his data before publication. We are also grateful to L. Allen of this Laboratory for preparing many of the targets used in this experiment and to W. S. Hall for preparation of most of the computer codes used for data reduction and analysis. We are indebted to S. G. Thompson for the Cf^{252} source used for calibration.

PHYSICAL REVIEW VOLUME 129, NUMBER 5 1 MARCH 1963

Elastic Scattering of Alpha Particles from Helium*

T. A. TOMBRELLO AND L. S. SENHOUSE
California Institute of Technology, Pasadena, California
(Received 1 October 1962)

The scattering of alpha particles from He^4 has been studied for laboratory energies between 3.8 and 12 MeV. Ten angular distributions have been measured over this range of energies as well as excitation curves at the center-of-mass angles 30.6°, 40°, 54.8°, 70.2°, and 90°. A phase-shift analysis of these data has been made and is compared to previously published results.

INTRODUCTION

EXPERIMENTAL investigation of the scattering of alpha particles from He^4 was first made by Rutherford and Chadwick[1] using alpha particles from natural sources. Further measurements by Chadwick[2] and by Blackett and Champion[3] showed that the scattering exhibited the strong deviations from classical Coulomb scattering that had been predicted by Mott.[4]

In recent years, the availability of intense alpha-particle beams from accelerators and the development of improved detection techniques have allowed precise experimental data to be taken for bombarding energies between 150 keV and 38.4 MeV.[5–9] Our purposes in seeking to add to this rather extensive body of data were to cover the previously untouched energy region between 9 and 12 MeV and to resolve certain small disagreements between published results near 7 MeV.[7,10,11] These disagreements, though small in themselves, are

* Supported in part by the Joint Program of the Office of Naval Research and the U. S. Atomic Energy Commission.

[1] E. Rutherford and J. Chadwick, Phil. Mag. 4, 605 (1927).
[2] J. Chadwick, Proc. Roy. Soc. (London) A128, 120 (1930).
[3] P. M. S. Blackett and F. C. Champion, Proc. Roy. Soc. (London) A130, 380 (1931).
[4] N. F. Mott, Proc. Roy. Soc. (London) A126, 259 (1930). A summary of early experimental work is given by J. A. Wheeler, Phys. Rev. 59, 16 (1941).
[5] E_α=0.15 to 3 MeV: N. P. Heydenburg and G. M. Temmer, Phys. Rev. 104, 123 (1956).
[6] E_α=2.5 to 5.5 MeV: J. L. Russell, G. C. Phillips, and C. W. Reich, Phys. Rev. 104, 135 (1956).
[7] E_α=5.0 to 9 MeV: C. M. Jones, G. C. Phillips, and P. D. Miller, Phys. Rev. 117, 525 (1960).
[8] E_α=12 to 23 MeV: R. Nilson, R. O. Kerman, G. R. Briggs, and W. K. Jentschke, Phys. Rev. 104, 1673 (1956); R. Nilson, W. K. Jentschke, G. R. Briggs, R. O. Kerman, and J. N. Snyder, *ibid.* 109, 850 (1958).
[9] E_α=23 to 38.4 MeV: D. J. Bredin, W. E. Burcham, D. Evans, W. M. Gibson, J. S. C. McKee, D. J. Prowse, J. Rotblat, and J. N. Snyder, Proc. Roy. Soc. (London) A251, 143 (1959).
[10] N. Berk, F. E. Steigert, and G. L. Salinger, Phys. Rev. 117, 531 (1960).
[11] J. R. Dunning, A. M. Smith, and F. E. Steigert, Phys. Rev. 121, 580 (1961).

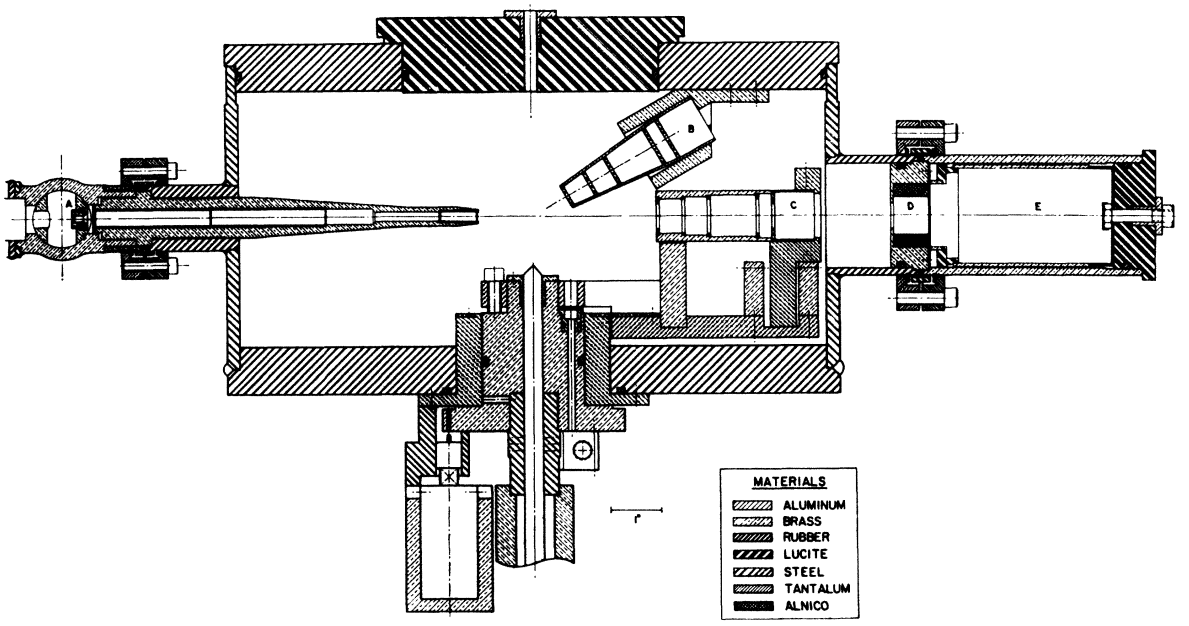

FIG. 1. A cross-section view of the gas scattering chamber. The entrance foil holder is shown at (A); the monitor counter is at (B); the moving counter (positioned at 0°) is at (C); the holder for the exit foil and magnets is at (D); and the Faraday cup is at (E).

important in applications where the energy dependence of the wave function for the relative motion of two alpha particles is needed—as in the recent calculations of Griffy and Biedenharn[12] and of Beckner *et al.*[13]

APPARATUS

The ONR tandem accelerator was used as a source of the singly and doubly charged alpha-particle beams that were used in this experiment, following a procedure developed by the High Voltage Engineering Corporation. Singly charged ions are accelerated to approximately 600 keV, focused, and passed through a helium exchange canal. The resulting neutral component of the beam is introduced into the tandem accelerator and is ionized at the central terminal. The desired ion beam is then selected by magnetic analysis; in this case, singly charged helium ions were used for bombarding energies between 3.8 and 6 MeV, and doubly charged ions were used for all higher energies.

The scattering chamber is shown in Fig. 1. The scattering volume is isolated from the high-vacuum system by a 2500-Å nickel foil before the beam collimator, and by a 10 000 Å nickel foil in front of the Faraday cup. An adequate vacuum is maintained in the Faraday cup by connecting it to the main pumping station through a short 1-in.-diam manifold. The chamber was filled with 99.99% pure helium to a pressure of approximately 10 cm, as measured with a manometer of *n*-butyl sebacate (density measured to be 0.927 ± 0.003 g/ml) and read with a cathetometer to an accuracy of ±0.01 cm. The significant contaminants contained in the gas were kept to a very low level by a liquid-nitrogen-cooled charcoal trap in the bottom of the chamber.

The temperature was monitored with a mercury-filled thermometer that was inserted through the top of the chamber to within an inch of the beam. Variation of beam intensities over a wide range has shown that errors in cross-section measurements due to local beam heating may be neglected.

The beam current was integrated with an Eldorado model CI-110 current integrator, which was calibrated frequently with a precision current source. Since the calibration current was chosen to be the same as the beam current, the effects of leakage currents in the integrator circuit were minimized. The precision of this measurement is about $\pm0.5\%$. Electrons produced by the beam striking the exit foil were prevented from reaching the Faraday cup by means of a permanent magnet and by an electrostatic suppression ring, which was held at -300 V. The Faraday cup itself was maintained at a positive potential to prevent loss of electrons. The proper operation of the beam collection system was demonstrated by scattering alpha particles from argon[14] and by scattering protons from hydrogen.[15]

The alignment of the beam collimator and the collimator of the moving counter was determined optically,

[12] T. A. Griffy and L. C. Biedenharn, Nucl. Phys. **15**, 636 (1960).

[13] E. H. Beckner, C. M. Jones, and G. C. Phillips, Phys. Rev. **123**, 255 (1961).

[14] C. M. Jones, Ph.D. thesis, Rice University, 1961 (unpublished).

[15] D. J. Knecht, S. Messelt, E. D. Berners, and L. C. Northcliffe, Phys. Rev. **114**, 550 (1959).

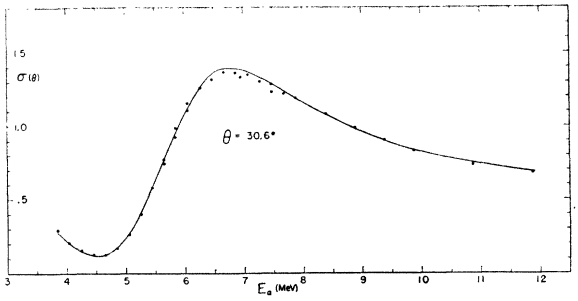

FIG. 2. Excitation curve for α-α scattering at the center-of-mass angle $\theta=30.6°$. The cross section is in the center-of-mass system and is given in barns/steradian. The solid curve is that given by the derived phase shifts. The energy scale is in the laboratory system and is expressed in MeV.

and the counter slits were measured with a traveling microscope. The dimensions of the counter collimator were chosen so as to minimize the second-order geometrical corrections at the forward angles.[16] This counter has an angular resolution of $\pm 1°$ and can cover the range of laboratory angles between 10° and 170°. Observation angles can be set with an accuracy better than $\pm 0.1°$. The scattered particles were detected with a 1-mm-thick lithium-drifted solid-state detector, which has an energy resolution of $\sim 1.5\%$ for 8.8-MeV alpha particles. The effect of multiple scattering was checked by varying the chamber pressure from 2 to 30 cm; for the pressure used (~ 10 cm) this effect was negligible even at the most forward angle considered in this experiment.

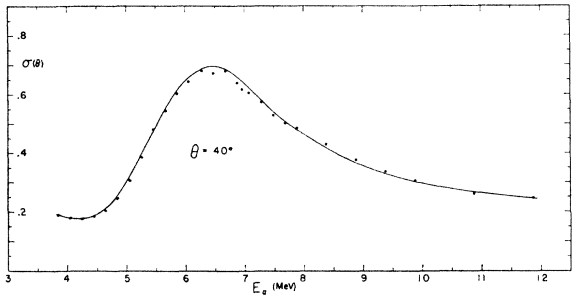

FIG. 3. Excitation curve for the center-of-mass angle, $\theta=40°$. The units and symbols are the same as those of Fig. 2.

A detector fixed at 30° to the incident beam was used as a monitor. This detector was a surface-barrier type with an energy resolution of $\sim 1\%$.

The signals from the detectors were fed through Tennelec model 100A charge-sensitive, cascode preamplifiers and Hamner model N328 linear amplifiers. Spectra from the moving counter were recorded with an RIDL 400-channel analyzer. The pulses from the monitor counter were recorded using a discriminator and a scaler.

[16] G. Breit, H. M. Thaxton, and C. Eisenbud, Phys. Rev. **55**, 1018 (1939); H. R. Worthington, J. N. McGruer, and D. E. Findley, *ibid.* **90**, 899 (1953).

EXPERIMENT

The experimental data consist of five excitation curves at center-of-mass angles 30.6°, 40°, 54.8°, 70.2°, and 90°, which are shown in Figs. 2–6, and ten angular distributions, which are shown in Figs. 7–11. These results are in good agreement with previously published data in the regions where direct comparison is possible.

The beam current and target pressure were adjusted in such a way as to keep the analyzer dead time correction below a few percent. This correction was determined by comparison of the "live-time" scaler of the analyzer with an accurate timer. Since this correction

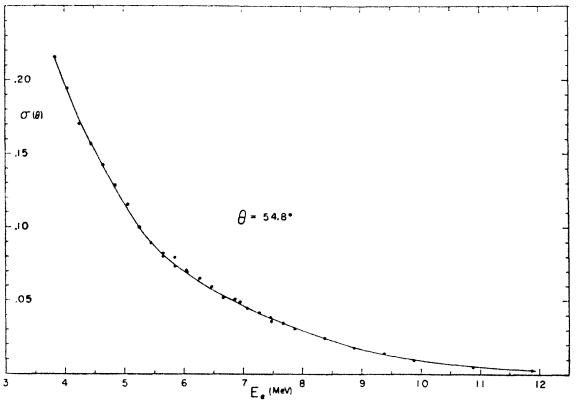

FIG. 4. Excitation curve for the center-of-mass angle, $\theta=54.8°$. The units and symbols are the same as those of Fig. 2.

was itself small and the beam current was steady, any error it might contain is reduced still further.

The energy scale given has an uncertainty of ± 35 keV. This error includes the uncertainty in the entrance foil thickness, as well as that arising in the magnetic analyzing system.

The estimated root-mean-square uncertainty of the cross-section measurements due to all error sources except counting statistics is less than $\pm 4\%$. Because of the range in the magnitude of the cross section, the statistical uncertainty varies markedly with the energy and observation angle. The range of this uncertainty for several of the angles studied is indicated in Table I.

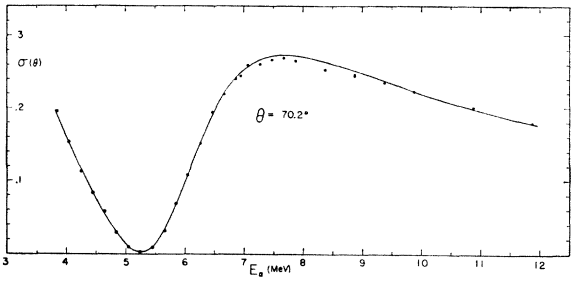

FIG. 5. Excitation curve for the center-of-mass angle, $\theta=70.2°$. The units and symbols are the same as those of Fig. 2.

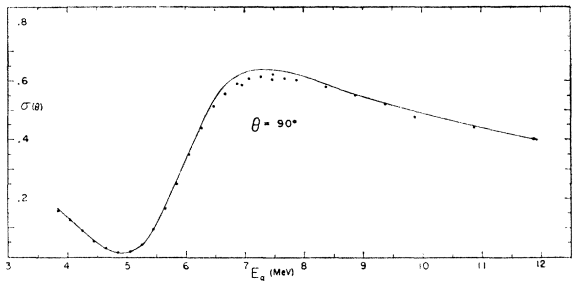

FIG. 6. Excitation curve for the center-of-mass angle, $\theta=90°$. The units and symbols are the same as those of Fig. 2.

TABLE I. Variation in counting statistics for several angles.

$\theta_{c.m.}$	Counting statistics (%)
30.6°	0.3–0.7
40°	0.5–1.0
54.8°	1.5–3.0
70.2°	1.0–1.5
90°	0.7–1.5

PHASE-SHIFT ANALYSIS

The scattering of alpha particles from He^4 at low energies represents one of the simplest examples of nuclear scattering. The spinless nature of the two particles and the absence of other open channels should

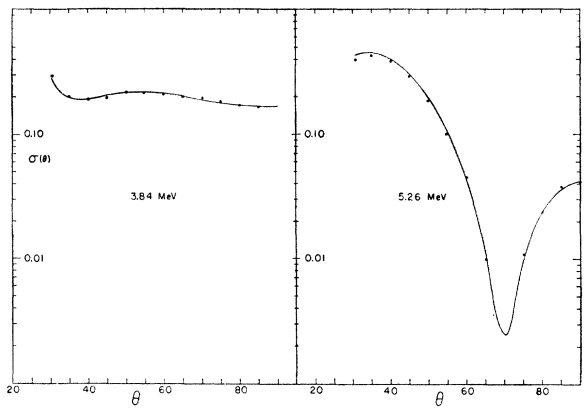

FIG. 7. Differential cross section for α-α scattering at laboratory energies of 3.84 and 5.26 MeV. The center-of-mass scattering angle, θ, is in degrees, and the cross section, σ, is in the center-of-mass system and is measured in barns/steradian. The solid lines were calculated from the derived phase shifts that are given in Table II.

permit an unambiguous phase-shift analysis based entirely upon a knowledge of the differential cross section as a function of the bombarding energy.[17] The fact that the target nucleus and the incident particle are identical bosons allows only symmetric terms in the wave function and thus further simplifies the analysis by limiting the angular momentum to even values. For bombarding energies below 20 MeV, this reduces the scattering analysis to a determination of the phase shifts for S, D, and G partial waves.

The formula for the differential cross section in the center-of-mass system in terms of the nuclear phase

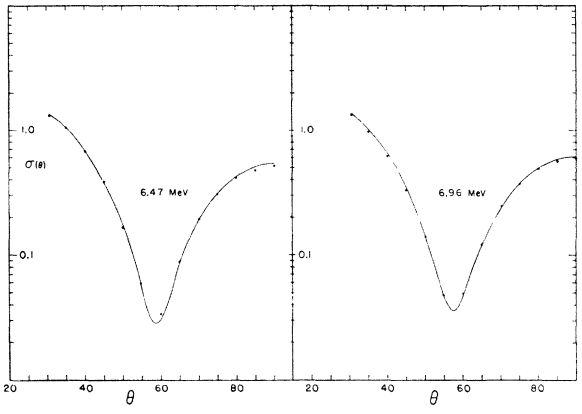

FIG. 8. The differential cross section for laboratory energies 6.47 and 6.96 MeV. The units and symbols are the same as those of Fig. 7.

shifts is[18]:

$$\sigma(\theta)=|f(\theta)|^2=\left|\frac{-\eta}{2k}\csc^2\left(\frac{\theta}{2}\right)\exp\left[i\eta\ln\csc^2\left(\frac{\theta}{2}\right)\right]\right.$$
$$-\frac{\eta}{2k}\csc^2\left(\frac{\pi-\theta}{2}\right)\exp\left[i\eta\ln\csc^2\left(\frac{\pi-\theta}{2}\right)\right]$$
$$\left.+\frac{2}{k}\sum_{L=0,2,4,\cdots}^{\infty}(2L+1)\sin\delta_L\times\exp[i(2\alpha_L+\delta_L)]P_L(\cos\theta)\right|^2,$$

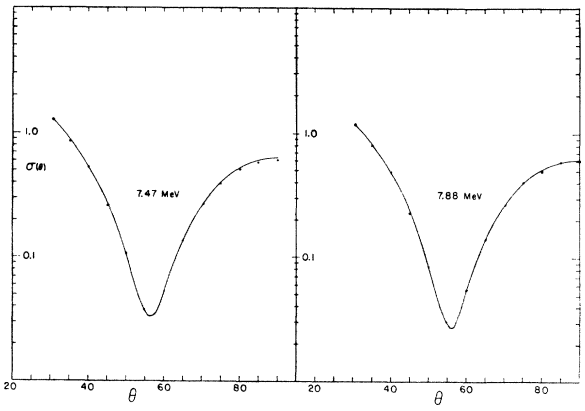

FIG. 9. The differential cross section for laboratory energies 7.47 and 7.88 MeV. The units and symbols are the same as those of Fig. 7.

[17] L. Puzikov, R. Ryndin, and J. Smorodinsky, Nucl. Phys. 3, 436 (1957).

[18] N. F. Mott and H. S. W. Massey, *The Theory of Atomic Collisions* (Oxford Press, New York, 1953).

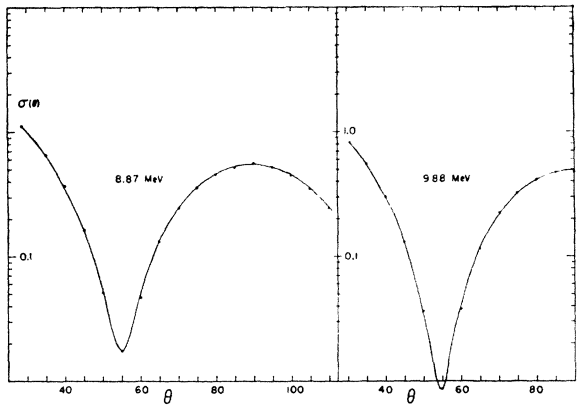

FIG. 10. The differential cross section for laboratory energies 8.87 and 9.88 MeV. The units and symbols are the same as those of Fig. 7.

where

$$\eta=\frac{4e^2}{\hbar v},\quad \alpha_L=\sum_{s=1}^{L}\tan^{-1}\left(\frac{\eta}{s}\right),\quad \alpha_0=0,$$

v is the relative velocity of the two alpha particles, k is the wave number, and θ is the center-of-mass scattering angle.

The phase-shift analysis problem has been programmed for the Burroughs 220 computer. The extraction of a set of phase shifts was obtained by using successively two separate numerical procedures; this was done in the hope that if this method allowed a significant saving in computing time for the present analysis, it might prove useful in more complicated cases.

The first step in the analysis is similar to that used by Reich[19] for the analysis of the scattering of protons from carbon. Consider an expansion of the experimental cross section at a given angle in terms of the cross section calculated from a trial set of phase shifts δ_0, δ_2, $\cdots$, $\delta_{2(N-1)}$ plus a linear correction term involving increments of the starting set of phase shifts, $\Delta\delta_j$.

$$\sigma_{\text{exp}}(\theta_i)=\sigma_{\text{calc}}(\theta_i,\delta_0,\delta_2,\cdots)+\sum_{j=0}^{2(N-1)}\frac{\partial\sigma}{\partial\delta_j}(\theta_i,\delta_0,\cdots)\Delta\delta_j. \quad (1)$$

The partial derivatives of the cross section may be calculated exactly:

$$(\partial\sigma/\partial\delta_j)(\theta_i,\delta_0,\cdots)=(4/k)(2j+1)P_j(\cos\theta_i)$$
$$\times\{\cos 2(\alpha_j+\delta_j)\ \text{Re}[f(\theta_i)]+\sin 2(\alpha_j+\delta_j)\ \text{Im}[f(\theta_i)]\}.$$

For convenience, let us introduce the following notation:

$$(\partial\sigma/\partial\delta_j)(\theta_i,\delta_0,\cdots)=a_{ij},$$
$$\sigma_{\text{exp}}(\theta_i)-\sigma_{\text{calc}}(\theta_i,\delta_0,\cdots)=Z_i,$$

and

$$\Delta\delta_j=x_j.$$

[19] C. W. Reich, G. C. Phillips, and J. L. Russell, Phys. Rev. **104**, 143 (1956).

Then Eq. (1) can be rewritten as

$$\sum_{j=0}^{2(N-1)}a_{ij}x_j=Z_i. \quad (2)$$

The maximum value of j is determined by the maximum number of phase shifts considered, while that of i is determined by the number of pieces of data at this energy. In general, we have more data than phase shifts, and the linear system given by (2) is overdetermined. Applying the least-squares criterion to this set of equations reduces it to an $N\times N$ set that is easily solved.

$$\frac{\partial\chi^2}{\partial x_p}=\frac{\partial}{\partial x_p}\left[\sum_i\left(Z_i-\sum_k a_{ik}x_k\right)^2\right]=0$$

yields

$$\sum_{i,k}a_{ip}a_{ik}x_k=\sum_i a_{ip}Z_i.$$

If we again modify our notation by defining

$$\alpha_{pk}=\textstyle\sum_i a_{ip}a_{ik},$$
$$\beta_p=\textstyle\sum_i a_{ip}Z_i,$$

then the $N\times N$ system of linear equations is just

$$\textstyle\sum_k \alpha_{pk}x_k=\beta_p.$$

The program iterates this process until the x_k are less than some prescribed value, as one would do in using Newton's method to find the zeros of a function.

At this point the program has produced a good fit to the data, and the set of phase shifts obtained are fairly close to their final values. A final set of phase shifts is obtained in the usual manner by minimizing the function

$$f(\delta_0,\delta_2,\delta_4)=\sum_i\frac{Z_i^2}{[\nu_i\sigma_{\text{exp}}(\theta_i)]^2}$$

with respect to the set of phase shifts, where $\nu_i\sigma_{\text{exp}}(\theta_i)$ is the root-mean-square uncertainty in the measurement

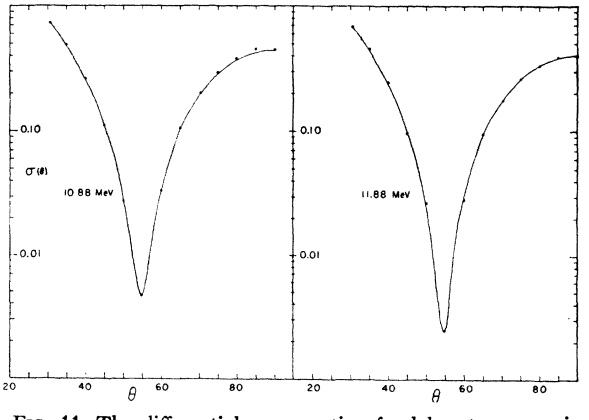

FIG. 11. The differential cross section for laboratory energies 10.88 and 11.88 MeV. The units and symbols are the same as those of Fig. 7.

TABLE II. The phase shifts derived from the angular distributions. The quantity ϵ is defined in the text.

E_α (MeV)	δ_0	δ_2	δ_4	ϵ
3.84	114.1°±1°	7.5°±1°	−0.1°	0.87
5.26	96.6°±2°	37.5°±2°	0.2°	2.85
6.47	79.5°±2°	80.8°±2°	−0.1°	1.40
6.96	75.9°±3°	92.7°±3°	−0.1°	1.32
7.47	71.4°±4°	102.1°±4°	0°	1.16
7.88	68.0°±4°	107.5°±4°	0°	0.59
8.87	59.4°±4°	113.8°±3°	0°	0.77
9.88	51.6°±4°	115.2°±2°	0°±1°	0.88
10.88	45.6°±4°	116.3°±2°	0°±1°	0.76
11.88	41.0°±4°	114.9°±2°	0°±1°	1.02

at θ_i. A measure of the fit obtained is given by

$$\epsilon=[f_{\min}/(n-m)]^{1/2},$$

where n is the number of observations, m is the number of phase shifts used, and $f_{\min}$ is the minimum of the function $f(\delta_0,\delta_2,\delta_4)$. A value of ϵ of the order of one is commensurate with the accuracy of the experimental data.[8] The values of the phase shifts obtained for the ten angular distributions are given in Table II and in Fig. 12. The additional points shown in Fig. 12 are based on the analysis of the five-point angular distributions that were taken from the excitation curves.

The phase shifts for alpha-particle energies between 3.8 and 6 MeV are in excellent agreement with those obtained by Russell.[6] Below 9 MeV, the S-wave phase shift agrees well with that of Jones,[7] but values of the D-wave phase shift show increasing disagreement with increasing energy. This disagreement is, however, within the uncertainty quoted for his results. The phase shifts at 7.56 MeV of Berk *et al.*, and at 7.78 MeV of Dunning *et al.*, are also in excellent agreement with our values. The point of Dunning at 6.43 MeV agrees reasonably well, while his point at 6.84 MeV does not.

Figure 13 shows the present phase shifts together with the results of Heydenburg and Temmer[5] and those of Nilson *et al.*[8] All the data are consistent except for the two points of Nilson at 12.3 and 15.2 MeV. An

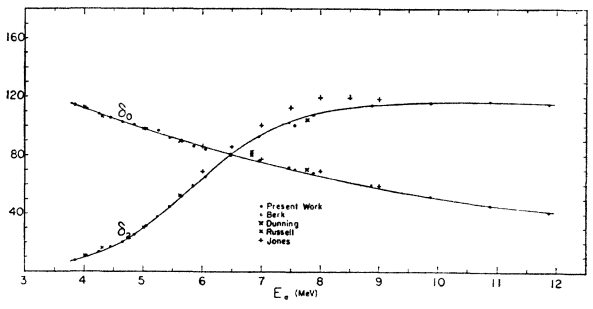

FIG. 12. The phase shifts in degrees for α-α scattering for bombarding energies between 3 and 12 MeV. In addition to the present results, results from the Rice and Yale groups are shown. The solid lines serve only to connect the points. (Dunning's point at 6.43 MeV is not shown. His parameters for this energy are $\delta_0=82.5°$, $\delta_2=77.5°$.) (Only scattered points of Jones *et al.* are given in order to show the trend of their results.)

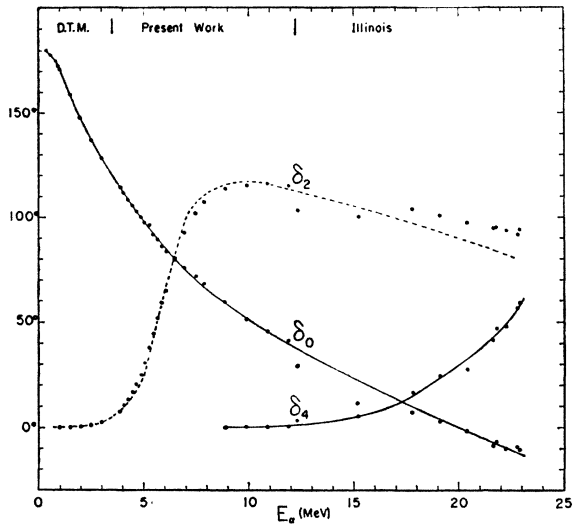

FIG. 13. The phase shifts for α-α scattering for bombarding energies up to 23 MeV. In addition to the present results, the results of Heydenburg and Temmer (D.T.M.) and of Nilson *et al.* (Illinois) are shown. The solid lines serve only to connect the points, while the broken line is given by the single-level parameterization of δ_2 that is discussed in the text.

analysis of their data at these points using our program yielded the same set of parameters that they obtained, and the extrapolated values of our excitation curves at 12.3 MeV agree with their data to within our combined errors.

The disagreement of these points with the line connecting the present data with their data above 17 MeV is barely outside the combined errors given. Part of the difficulty in this energy region can be explained by Fig. 14. Contours of

$$\chi^2=\sum_{i=1}^{13}\left[\frac{\sigma_{\exp}(\theta_i)-\sigma_{\text{calc}}(\theta_i)}{\sigma_{\exp}(\theta_i)}\right]^2$$

are plotted versus δ_0 and δ_2 for several values of δ_4 at 9.88 and 11.88 MeV. At the lower energy, the two solutions are well separated, but at 11.88 MeV one solution is seen to be at ($\delta_0=41°$, $\delta_2=115°$, $\delta_4=0°$) while the other is at (35°, 90°, 4°). Thus, in this energy region one can find two solutions which have different values of δ_2, but which differ only slightly in δ_0 and δ_4. The identification of the "correct" solution is possible only if it is followed from lower energies where the two minima are more clearly separated; the "wrong" solution can be rejected in this manner on the basis of its energy dependence.

The two solutions obtained by Nilson *et al.* at 12.3 MeV are (29°±4°, 103°±8°, 3°±1.5°) and (40.2°±4°, 102°±8°, 0°±1°). Small differences between their data and ours have produced sufficient distortion of the contours that the two minima have been displaced toward one another in the δ_2 direction. It is difficult to see exactly how this displacement arises, but it may be

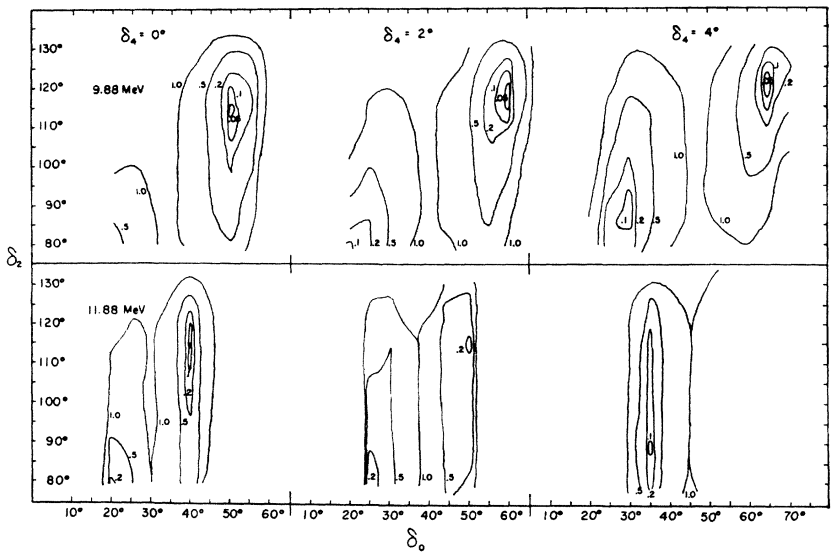

FIG. 14. Contours of

$$\chi^2=\sum_{i=1}^{13}\left[\frac{\sigma_{\exp}(\theta_i)-\sigma_{\text{calc}}(\theta_i)}{\sigma_{\exp}(\theta_i)}\right]^2$$

plotted versus δ_0 and δ_2 for several values of δ_4 at 9.88 and 11.88 MeV. A value of $\chi^2=0.05$ is equivalent to $\epsilon=1.8$.

traceable to the extra weight given in their analysis to the forward angle data or to the relatively large statistical errors in the cross section near $\theta=55°$. If the second solution rather than the first is assumed to be "correct," then most of the disagreement is removed at this energy. This explanation is, however, not possible at 15.2 MeV, where the two solutions are clearly separated. At this energy, the second solution is (60.8°, 104.5°, 0.2°).

A parameterization of δ_2 in terms of the single-level formalism is shown by the broken line in Fig. 13. The level parameters for the 2^+ state that were obtained in this manner are:

radius, $R=3.5\times10^{-13}$ cm,

reduced width, $\gamma_2^2=3.36$ MeV,

excitation energy, $E_x=3.18$ MeV,

ratio to the Wigner limit, $\theta_2^2=\gamma_2^2/(3\hbar^2/2\mu R^2)=1.27$.

These resonance parameters are virtually identical to those obtained by Jones. A better fit to the high-energy points can be obtained by choosing smaller values of the radius; however, this worsens the fit at lower energies and requires values of θ_2^2 that are significantly greater than one. Larger values of R allow a better fit at the lower energies, but produce extreme disagreement with the high-energy points.

Since these level parameters are chosen primarily as a compromise between the disagreements at high and low energies, and since the fit to the data is not impressive, it is possible to question whether such a parameterization has any significance. This possibility is further enhanced by the variety of level parameters that have been obtained for this level from other reactions.[20,21] Several of these sets of parameters are given in Table III.

An explanation of this failure of the single-level formula to describe the energy dependence of δ_0 [8] and δ_2 is given by Jones on the basis of the scalar α-α potential proposed by Russell. Since this potential has a repulsive core, another strong energy dependence is introduced in addition to that produced by the level or by the nuclear radius. As Jones indicated, this dependence would, if ignored, appear as an energy variation of the radius given by the single-level parameterization.

TABLE III. Level parameters obtained for the 2^+ state of Be^8.

Reaction	Radius (cm)	θ_2^2	Excitation energy (MeV)	Reference
$B^{10}(d,\alpha)Be^8$	4.5×10^{-13}	1.93	2.88	21
$Be^7(d,p)Be^8$	5.75×10^{-13}	0.64	2.90	20
$He^4(\alpha,\alpha)He^4$	3.5×10^{-13}	1.32	3.1	7
$He^4(\alpha,\alpha)He^4$	3.5×10^{-13}	1.27	3.18	This report

ACKNOWLEDGMENTS

The authors wish to acknowledge the fellowship aid from the Hughes Aircraft Company (L. S. S.) and the National Science Foundation (T. A. T.) during the course of this work. We also wish to thank Y. Cusson for making the lithium-drifted detector and Barbara Hinds for her help with the data reduction.

[20] R. W. Kavanagh, Nucl. Phys. 18, 492 (1960).
[21] P. B. Treacy, Phil. Mag. 44, 325 (1953).